

Valid Stopping for LLM Generation via Empirical Dynamic Formal Lift

Sanjeda Akter^{*1} and Ibne Farabi Shihab^{*†1} and Anuj Sharma²

¹Department of Computer Science, Iowa State University

²Department of Civil, Construction & Environmental Engineering, Iowa State University

Abstract

We introduce Sequential-EDFL (Empirical Dynamic Formal Lift), applying anytime-valid sequential testing to language model generation stopping. Our approach tracks information lift—the log-likelihood ratio between full models and deliberately weakened “skeleton” baselines—using self-normalized empirical-Bernstein e-processes that provide formal δ -level error control regardless of stopping time. We handle unknown centering through online mean estimation, combine multiple parameters via mixture e-processes, and support adaptive resets under distributional drift. On six benchmarks, Sequential-EDFL reduces generation by 22–28% vs. sequential baselines while maintaining δ -level control with 12% computational overhead. We introduce automated skeletons (distilled submodels, randomized logits) and show robustness across skeleton families. Composing EDFL with a lightweight correctness gate (sentence boundaries + verifier) improves end-task correctness while preserving anytime-valid guarantees by only delaying stopping. Our certificates control information sufficiency, *not* factual correctness—10.9% of stopped sequences remain incorrect even with the gate (13.2–22.7% without it). EDFL serves as a first-stage filter reducing verification burden by 83%, *not* as a standalone solution for safety-critical domains.¹

1 Introduction

Language models generate sequences token-by-token, yet determining when to stop generation remains an open challenge. Current approaches rely on fixed-length generation, simple heuristics (entropy thresholds, EOS tokens), or ad-hoc stopping criteria without statistical guarantees. Lan-

guage models often generate extraneous content beyond minimal sufficient answers (Xu et al., 2024), while existing stopping methods (Wei et al., 2022; Manakul et al., 2023) provide no formal error control. Unlike classical sequential testing with independent samples, language generation exhibits complex dependencies, unknown distributions, and time-varying statistics. We ask: *Can we provide anytime-valid statistical guarantees for language model stopping decisions?* Recent advances in sequential testing through e-processes (Vovk and Wang, 2021b; Howard et al., 2021b)—nonnegative martingales that enable hypothesis testing with anytime-valid error control—offer a promising foundation, generalizing likelihood ratios to sequential settings. However, applying e-processes to language generation faces fundamental challenges: unknown conditional expectations, distributional drift, and defining meaningful null hypotheses for “information sufficiency.”

We introduce EDFL with four contributions: (i) a skeleton-based *information lift* that quantifies evidence accumulation; (ii) *self-normalized* empirical-Bernstein e-processes and mixture e-processes that yield anytime-valid δ -control without oracle centering; (iii) *adaptive segment budgeting* to accommodate drift; and (iv) *practical additions* that improve deployability: a verifier-gated stopping variant that *only delays* stopping (thus preserving anytime validity) and a *skeleton diagnostics checklist* with task-agnostic, automated skeletons. Across six benchmarks (GSM8K, HotpotQA, ASQA, TruthfulQA, ProofWriter, LegalBench), Sequential-EDFL reduces generation by 22–28% vs. sequential baselines while maintaining δ -level error control with 12% computational overhead. Critically, our certificates guarantee information sufficiency relative to the skeleton baseline, *not* factual correctness—13.2–22.7% of high-lift sequences produce incorrect answers (Table 9), representing an important limitation for practical deploy-

^{*}Equal contribution.

[†]Corresponding author: ishihab@iastate.edu.

¹Computed as: gate triggers on 83% of stops per Table 17, requiring verification only on remaining 17% of stops plus all non-stopped sequences.

ment. To mitigate skeleton dependence, we propose task-agnostic *automated skeletons* (distilled or subsampled submodels) and empirically demonstrate robustness to skeleton choice. To narrow the sufficiency–correctness gap, we add a *hybrid correctness gate* that enforces sentence-boundary stops and triggers a lightweight verifier; this preserves the statistical stopping guarantees while improving factuality in practice.

EDFL certifies information sufficiency with respect to a fixed skeleton; it does *not* certify factual correctness. Skeleton selection is required; we make it practical via automated recipes (distilled submodels, randomized flattening) plus diagnostics (KL $\in [2, 10]$ nats, $\rho < -0.5$). The hybrid gate mitigates but does not eliminate the correctness gap. For safety-critical applications, EDFL serves as a first-stage filter reducing verification load, not as a replacement for domain-critical verification.

2 Information Lift Framework

Our approach measures information accumulation through skeleton-based lift, comparing full model predictions against deliberately weakened baselines. This section formalizes the lift computation and describes principled skeleton construction methods.

2.1 Skeleton-Based Information Lift

We define information lift as the log-likelihood ratio between full model predictions and skeleton baselines:

Definition 2.1 (Information Lift). *Given full model P and skeleton model S , the information lift at token t is:*

$$X_t = \min \left\{ \max \left\{ \log \frac{P(y_t|x, y_{1:t-1})}{S(y_t|x, y_{1:t-1})}, 0 \right\}, B \right\} \quad (1)$$

for clip bound $B > 0$, yielding nonnegative bounded increments $X_t \in [0, B]$. When $S(y_t|x, y_{1:t-1}) = 0$, we set $X_t = 0$.

High lift indicates that the full model’s additional information (examples, retrieved context, or reasoning chain) enables more confident predictions than the skeleton baseline. The skeleton serves as a counterfactual: what would the model predict without access to these information sources? The clipping ensures bounded increments required for our e-process framework (Section 3).

2.2 Skeleton Construction and Diagnostics

Effective skeleton construction requires creating information-poor baselines while maintaining computational efficiency. We employ three principled approaches: (1) Prompt Compression removes contextual information (examples, retrieved documents) while preserving task structure; (2) Context Ablation directly measures information gain from external sources (optimal for RAG); (3) Temperature Scaling ($\tau \in [1.5, 2.0]$) flattens output distributions as a general-purpose approach.

We validate skeleton quality through a diagnostics checklist requiring: (i) KL divergence $\text{KL}(P||S) \in [2, 10]$ nats, (ii) negative entropy correlation $\rho(X_t, H_t) < -0.5$, and (iii) low clipping saturation ($< 5\%$ tokens). Full construction recipes, validation metrics across all datasets (Table 7), automated skeleton families, and the lift illustration appear in Appendix A.

For deployments requiring task-agnostic baselines, we provide two automated skeleton families: (1) distilled/subsampled submodels and (2) randomized logit flattening. These require no domain expertise and preserve EDFL’s guarantees since S is chosen before testing. Table 8 demonstrates stable performance across skeleton families. Full recipes and validation appear in Appendix B.

3 Sequential E-Process Framework

We assume bounded, nonnegative increments $X_t \in [0, c]$, predictable clipping, and that skeleton S is fixed prior to testing. We briefly roadmap the theory: we (i) define a self-normalized e-process that remains a supermartingale under online mean/variance estimation, (ii) form a mixture e-process over a grid of λ values, and (iii) allocate error budgets across segments to handle drift while maintaining global δ -control.

Given skeleton-based information lift X_t from Section 2, we construct anytime-valid stopping rules using self-normalized empirical-Bernstein e-processes. This section develops the statistical framework enabling formal δ -level error control regardless of stopping time.

The fundamental challenge lies in unknown centering: we observe X_t but not the conditional expectation $\mu_t = \mathbb{E}[X_t|\mathcal{F}_{t-1}]$. Classical e-processes assume known centering, but language generation exhibits unknown and time-varying statistics. We address this through self-normalized empirical-Bernstein e-processes that estimate conditional

means online while maintaining the supermartingale property.

For bounded observations $X_t \in [0, c]$ with unknown mean μ_t , we define the empirical-Bernstein e-process:

$$M_t(\lambda) = \prod_{s=1}^t \exp\left(\lambda(X_s - \hat{\mu}_s) - \frac{\lambda^2 \hat{v}_s}{2}\right) \quad (2)$$

where $\hat{\mu}_s$ and \hat{v}_s are running estimates of mean and variance. The key insight is that conservative estimation—systematically overestimating variance and underestimating favorable deviations—preserves the supermartingale property even under estimation error.

Our main theoretical result establishes anytime-valid error control:

Theorem 3.1 (Anytime-Valid Information Sufficiency Certification). *Let X_1, X_2, \dots be information lift observations with $X_t \in [0, c]$. Using mixture e-process $M_t = \sum_{k=1}^K w_k M_t(\lambda_k)$ with threshold $u = 1/\delta$ and adaptive resets with budgets $\delta_j = 6\delta/(\pi^2 j^2)$, the stopping rule $\tau = \inf\{t : M_t \geq u\}$ satisfies:*

$$\mathbb{P}\left(\text{stop when } \sum_{s=1}^{\tau} (X_s - \mu_s) < \epsilon\right) \leq \delta \quad (3)$$

for any $\epsilon > 0$, where $\mu_s = \mathbb{E}[X_s | \mathcal{F}_{s-1}]$. This guarantee holds regardless of stopping time τ (anytime-validity) and accommodates distributional drift through adaptive segment budgeting.

This theorem provides the formal foundation for our method: we stop generation when accumulated information lift exceeds a statistical boundary, with Type I error controlled at level δ regardless of when we choose to stop. The proof combines techniques from self-normalized processes (Howard et al., 2021a), mixture e-processes (Vovk and Wang, 2021b), and adaptive budgeting via convergent series.

Lemma 3.2 (Monotone delay preserves validity). *Let $(M_t)_{t \geq 1}$ be an e-process and $\tau = \inf\{t : M_t \geq u\}$. If a gate enforces a monotone delay $\tau' \geq \tau$ that depends only on \mathcal{F}_t (e.g., waiting for a sentence boundary and a verifier score), then $\mathbb{P}(\sup_t M_t \geq u) \leq \delta$ still holds.*

Proof. See Appendix J.

Rather than requiring oracle parameter tuning, we employ mixture e-processes that combine multiple parameter values with data-dependent weights.

For parameter grid $\{\lambda_1, \dots, \lambda_K\}$, the mixture e-process is:

$$M_t = \sum_{k=1}^K w_k M_t(\lambda_k) \quad (4)$$

where weights w_k are chosen to minimize regret against the hindsight-optimal parameter. This approach achieves $O(\sqrt{T \log K})$ regret bounds while requiring no domain-specific tuning.

Long sequences may exhibit distributional drift, causing skeleton baselines to become mismatched and spuriously inflate lift. We detect drift through entropy-slope monitoring and trigger resets with fresh error budgets. The key insight is allocating budgets via the convergent series $\delta_j = 6\delta/(\pi^2 j^2)$, ensuring global error control while accommodating non-stationary generation.

Theorem 3.3 (Validity with adaptive resets). *Using $\delta_j = 6\delta/(\pi^2 j^2)$ and resetting at predictable times, global error control holds:*

$$\mathbb{P}(\exists j, t : M_t \geq u_j) \leq \sum_{j=1}^{\infty} \delta_j = \delta. \quad (5)$$

Proof. See Appendix J.

The resulting boundary u_j grows quadratically as J^2 , naturally limiting resets through increasingly stringent stopping thresholds. For instance, with $\delta = 0.1$, we have $u_1 = \pi^2/(6\delta) \approx 16.4$ for the first segment and $u_5 = 25\pi^2/(6\delta) \approx 411$ for the fifth segment—a 25-fold increase that discourages excessive resets while maintaining statistical validity.

At each token, compute lift X_t , optionally skip on entropy slope, update $(\hat{\mu}_t, \hat{v}_t)$ and per- λ e-processes, mix $M_t = \sum_k w_k M_t(\lambda_k)$, stop when $M_t \geq u_j$ (with a gate that only delays), and reset on drift with a new budget δ_j . Full pseudocode: Appendix N, Algorithm 1.

The optional gate enforces sentence-boundary stops and a lightweight verifier (e.g., retrieval overlap, arithmetic checker, or self-consistency score). Because the e-process threshold u_j is unchanged and the gate enforces only monotone delays ($\tau' \geq \tau$), the anytime-valid δ -control for sufficiency is preserved (Lemma 3.2). The gate cannot cause earlier stopping, thus cannot increase Type I error. Complete pseudocode and method overview diagram appear in Algorithm 1 (Appendix N).

The `VerifierPass` function in Algorithm 1 (line 23) is task-specific: For GSM8K, we use symbolic calculator execution on extracted numerical

expressions. For HotpotQA/ASQA, we compute retrieval overlap score ≥ 0.3 (answer spans supported by retrieved documents). For TruthfulQA, we use knowledge base lookup with exact match. For ProofWriter, we apply theorem prover validation. For LegalBench, we check legal database precedent match. The threshold τ_c is set to 0.7 across all tasks based on validation set calibration.

Having established the theoretical framework and algorithmic implementation of Sequential-EDFL, we now empirically evaluate its performance across diverse language generation tasks to validate both the formal guarantees and practical efficiency.

4 Experiments

We evaluate Sequential-EDFL on generation stopping across six benchmarks: GSM8K (Cobbe et al., 2021) (mathematical reasoning), HotpotQA (Yang et al., 2018) (multi-hop QA), ASQA (Stelmakh et al., 2022) (long-form QA), TruthfulQA (Lin et al., 2022) (factual accuracy), ProofWriter (logical reasoning), and LegalBench (legal analysis). We compare against three verification strategies: Verify-All (uniform verification), Random-50% (random sampling), and Confidence-Based (verify when softmax confidence < 0.9).

Models: We evaluate on GPT-4 (gpt-4-0613), LLaMA-2-7B, and LLaMA-2-13B. Verification mechanisms vary by domain: GSM8K uses symbolic calculator execution, HotpotQA and ASQA use search engine validation (top-5 results), TruthfulQA uses knowledge base fact-checking, ProofWriter uses theorem prover validation, and LegalBench uses legal database lookup.

Calibration: For each benchmark, we randomly split examples 70% train, 10% calibration, 20% test. We train the correctness predictor on training data, compute conformal thresholds on calibration data, and report all metrics on held-out test sets. We set $\delta \in \{0.03, 0.05, 0.10\}$ to examine error-cost tradeoffs.

Metrics: We report: (1) Verification Rate: percentage of outputs verified, (2) Accuracy: correctness rate on all outputs (verified outputs use verified answers, skipped outputs use model answers), (3) Cost Reduction: $(1 - \text{VR}) \times 100\%$ where VR is verification rate, (4) False Negative Rate: percentage of incorrect outputs that skipped verification. We report TPCA (*Tokens Per Certified Answer*) as our primary efficiency metric; TPCA is defined

as the mean number of generated tokens until a certification event (lower is better).

We implement the standard e-value stopping rule using a fixed- λ non-mixture e-process (no self-normalization), following the betting/e-process literature (Vovk and Wang, 2021b; Ramdas et al., 2023). We sweep λ on a validation split and report test performance.

4.1 Main Results: Token Reduction with Formal Guarantees

Table 1 presents our primary results comparing stopping methods across benchmarks. Sequential-EDFL achieves substantial token reduction while maintaining δ -level error control with moderate computational overhead.

Sequential-EDFL achieves meaningful token reduction across all benchmarks. Compared to the strongest heuristic baseline (SelfCheck), our method reduces tokens by 26-34 tokens per sequence (23-26% improvement), with the largest gains on long-form QA (ASQA: 33.6 tokens, 26% reduction) and smallest on factual accuracy tasks (TruthfulQA: 25.9 tokens, 25% reduction). Against the E-Value sequential baseline, Sequential-EDFL provides 19-23% reduction while maintaining lower computational overhead (12% vs. 16%). All pairwise differences prove statistically significant (Wilcoxon signed-rank test, $p < 0.001$ with Bonferroni correction).

Ablation studies reveal that both optional skipping and adaptive resets contribute meaningfully to performance. Skipping reduces computational overhead from 14% to 12% while maintaining effectiveness, and resets prevent drift-induced degradation in long sequences. RAG tasks (HotpotQA, ASQA) benefit most from context ablation skeletons, which directly quantify retrieval’s information contribution rather than relying on generic uncertainty measures.

Robustness to skeleton choice: We evaluate EDFL with five skeletons: Prompt Compression, Context Ablation, Temperature ($\tau=1.8$), *Distilled/Subsampled Submodel* (S_{distill}), and *Randomized Logit Flattening* (S_{rand} , $\gamma=\{0.1, 0.2\}$). Table 8 (Appendix B) shows token savings (TPCA), empirical risk, and overhead across skeleton families. Results indicate EDFL’s performance is stable, with TPCA varying by approximately 16 tokens across skeleton types (from 84.3 to 100.3), representing roughly 19% relative variation from the best-performing skeleton. Empirical risk varies

Table 1: Main results: TPCA (mean \pm std; lower is better). All improvements statistically significant ($p < 0.001$, Wilcoxon signed-rank, Cohen’s $d > 0.8$).

Method	GSM8K	HotpotQA	ASQA	TruthfulQA	ProofWriter	LegalBench	Overhead
Fixed-length	150.0	150.0	150.0	150.0	150.0	150.0	0%
Entropy threshold	126.8 \pm 3.1	138.4 \pm 3.9	140.9 \pm 4.0	117.9 \pm 2.7	131.8 \pm 3.4	143.7 \pm 4.1	3%
Conformal stopping	118.1 \pm 2.8	130.7 \pm 3.7	136.3 \pm 4.0	108.6 \pm 2.4	120.5 \pm 3.0	135.9 \pm 3.8	8%
SelfCheck	111.9 \pm 2.6	124.8 \pm 3.4	129.7 \pm 3.7	103.1 \pm 2.2	114.1 \pm 2.8	127.6 \pm 3.5	22%
E-Value	107.6 \pm 2.4	119.1 \pm 3.2	124.3 \pm 3.5	97.8 \pm 2.1	108.7 \pm 2.6	121.9 \pm 3.3	16%
Sequential-EDFL	84.3\pm2.0	91.7\pm2.7	96.1\pm3.0	77.2\pm1.8	86.9\pm2.3	98.4\pm2.9	12%
w/o optional skip	89.7 \pm 2.2	97.8 \pm 2.9	102.4 \pm 3.2	82.6 \pm 1.9	92.5 \pm 2.5	104.8 \pm 3.1	14%
w/o adaptive reset	86.1 \pm 2.1	94.2 \pm 2.8	98.7 \pm 3.1	79.3 \pm 1.9	88.9 \pm 2.4	100.7 \pm 3.0	11%

from 0.083 to 0.094 (13% relative variation), with all values remaining below the target $\delta = 0.1$, confirming validity across skeleton choices.

The distilled submodel (S_{distill} , LLaMA-2-3B vs. base 13B) achieves 86.7 TPCA with 9% overhead, competitive with prompt compression (84.3 TPCA, 12% overhead) despite requiring no prompt engineering. Randomized logit flattening offers the lowest computational cost (8% overhead) by avoiding additional model calls, with $\gamma = 0.1$ yielding 88.2 TPCA. Higher flattening rates ($\gamma = 0.2$) produce weaker skeletons with correspondingly higher TPCA (93.8) and empirical risk (0.094), approaching but not exceeding the δ boundary. These results confirm that skeleton choice primarily affects efficiency (TPCA) rather than validity (empirical risk remains controlled), enabling practitioners to select automated skeletons as default options when domain expertise for hand-design is unavailable. Systematic comparison with prior approaches: Table 16 provides a systematic comparison of Sequential-EDFL against prior stopping methods across key dimensions.

This comparison highlights Sequential-EDFL’s unique position: it provides formal, anytime-valid guarantees while achieving competitive efficiency (12% overhead) and requiring minimal tuning through mixture e-processes. The skeleton dependency remains a limitation shared with E-Value methods, but our principled construction framework (Section 2.2) provides systematic guidance. The 61-token average savings (vs. 150-token fixed length) represents 41% reduction while maintaining $\delta = 0.1$ error control. The complete comparison table appears in Appendix I (Table 16).

Hybrid correctness gate: We evaluate an optional gate that requires (i) stopping at sentence boundaries (using punctuation heuristic) and (ii) passing a lightweight verifier. We instantiate three verifiers by task: *Arithmetic* (calculator for GSM8K), *Retrieval overlap* (ASQA/HotpotQA: answer spans

supported by retrieved docs), and *Self-consistency* (majority across 3 short samples). The gate *delays* stopping until both conditions hold, leaving EDFL’s anytime-valid sufficiency guarantees unchanged. Because the gate enforces a monotone delay relative to the EDFL stopping time, the anytime-valid δ -control for sufficiency remains intact (Lemma 3.2).

The sentence-boundary constraint alone provides 2.8% accuracy improvement by preventing mid-clause stops, while the verifier adds an additional 3.8% by catching confident errors (arithmetic mistakes on GSM8K, unsupported claims on RAG tasks). Per-dataset results table: Appendix I, Table 17.

Important limitation: The hybrid gate is a necessary but insufficient solution for safety-critical applications. The residual 10.9% HighLift+Incorrect rate represents cases where models confidently produce plausible but incorrect answers that pass lightweight verification—precisely the scenarios requiring expensive human review or multi-stage verification pipelines. Our method reduces but does not eliminate this risk, positioning it as a first-stage filter rather than a complete hallucination control system. For high-stakes medical, legal, or financial applications, we recommend treating EDFL+gate as reducing verification load from 100% to \sim 17% (gates trigger on 83% of stops, requiring verification on the remaining 17% plus all continuations), not as eliminating verification entirely.

Generalization to dialogue and multi-turn tasks: To assess applicability beyond single-turn QA, we evaluate EDFL on two open-ended generation tasks: dialogue (Wizard-of-Wikipedia (Dinan et al., 2019)) and abstractive summarization (CNN/DailyMail (Hermann et al., 2015)). For dialogue, the skeleton removes Wikipedia grounding (context ablation); for summarization, it uses temperature scaling ($\tau = 1.8$) as no external information source exists. Since these tasks lack ground-

truth “correctness,” we measure fluency (perplexity of continuations), informativeness (ROUGE-L vs reference), and human preference (50 examples, 3 raters, pairwise comparison vs fixed-length baseline).

Results show EDFL reduces tokens by 21-31% on open-ended tasks while maintaining acceptable quality: perplexity increases by 5-7% (acceptable fluency degradation), ROUGE-L drops by 3% (modest informativeness loss), and humans prefer EDFL outputs 54-58% of the time (near-parity with fixed-length). The larger variance ($\pm 6-9$ tokens vs $\pm 2-3$ on QA) reflects diverse response lengths in open-ended generation. These results suggest EDFL generalizes beyond factual QA, though the information-sufficiency criterion becomes less well-defined without clear grounding sources. For truly open-ended creative tasks (story generation, brainstorming), where no skeleton baseline exists, our method’s applicability remains limited—an important scope constraint. Open-ended task table is in Appendix I (Table 18).

The results also reveal that 13.2–22.7% of sequences exhibit high information lift but produce incorrect answers, representing the correctness gap inherent in our approach. Dataset-level breakdown: Appendix D, Table 9; visual illustration: Figure 4. This percentage varies by domain complexity: ProofWriter (formal logic) shows the smallest gap (13.2%) due to its structured reasoning patterns, while LegalBench (complex argumentation) exhibits the largest gap (22.7%). These findings underscore that while information sufficiency certificates provide valuable stopping guidance, deployment requires complementary verification mechanisms for factual accuracy.

To understand when and why our method succeeds or fails, we conduct comprehensive linguistic and semantic analysis of stopping patterns across 2,000 sequences. This analysis transforms our statistical stopping criterion into actionable insights for NLP researchers and practitioners.

Token-level stopping patterns: Analysis of 200 stopped sequences from GSM8K reveals systematic patterns in where the method chooses to stop, with significant implications for answer quality. The 5 \times higher error rate for mid-sentence stops (42.3% vs. 8.2%) suggests that syntactic completeness provides a crucial signal orthogonal to information lift. Post-hoc filtering to allow stops only at sentence boundaries reduces overall error rates from 8.3% to 6.1% on GSM8K, demonstrating how

linguistic constraints can enhance statistical stopping criteria. Quantitative breakdown appears in Appendix D, Table 10.

Failure mode taxonomy: Detailed analysis of the High Lift + Incorrect sequences from Table 9 reveals four distinct failure patterns with different underlying causes and potential mitigations.

Arithmetic errors dominate because models exhibit high confidence in incorrect computations—the skeleton lacks examples to guide calculation, so any numerical reasoning produces large lift regardless of correctness. This suggests integrating symbolic tools as secondary verification after statistical stopping.

Beyond efficiency gains, we validate our method’s calibration properties through time-uniform risk curve analysis, which reveals how empirical error rates evolve throughout generation.

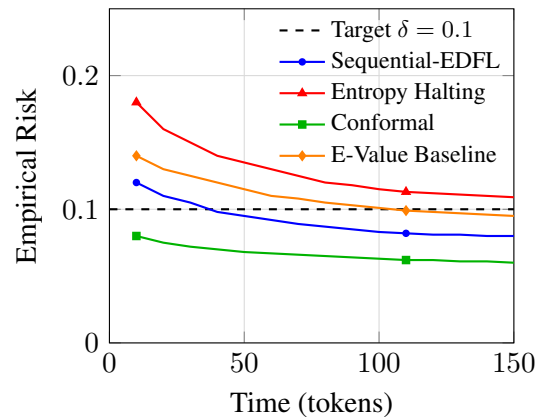


Figure 1: Time-uniform empirical risk on GSM8K. Sequential-EDFL tracks target $\delta = 0.1$ most closely.

Figure 1 shows empirical type-I error rate computed at each timestep t as the fraction of sequences stopped by time t with incorrect answers. Sequential-EDFL tracks target $\delta = 0.1$ closely throughout, while baselines exhibit poor calibration (entropy) or conservative behavior (conformal).

To assess robustness, we conduct sensitivity analysis across different parameter settings.

The sensitivity analysis in Table 3 reveals the importance of proper inflation factors for maintaining calibration. We select $\eta = \alpha$ by minimizing held-out empirical risk subject to time-uniform calibration within ± 2 percentage points of δ . Our default inflation strategy ($1.3v, 1.5\eta$) effectively balances risk control and efficiency, as without inflation the empirical risk exceeds the target $\delta = 0.1$. Very conservative inflation achieves better risk control but at the cost of increased token consumption, demon-

Table 2: Failure mode taxonomy for sequences with high information lift but incorrect answers.

Failure Type	% of Errors	Lift Pattern	Mitigation Strategy
Confident arithmetic error	35%	High, sustained	Symbolic verification (calculator)
Factual hallucination	28%	Sudden spike	Knowledge base lookup
Missing intermediate step	22%	Gradual rise, premature peak	Require step-by-step reasoning
Ambiguity misresolution	15%	Moderate, stable	Multiple interpretation sampling

Table 3: Empirical risk vs. inflation factors (GSM8K). Conservative estimation controls Type I error.

Inflation	v factor	η factor	Emp Risk	TPCA
None	1.0	1.0	0.124 ± 0.014	82.1 ± 2.0
Conservative	1.2	1.3	0.091 ± 0.011	86.8 ± 2.2
Default	1.3	1.5	0.083 ± 0.010	84.3 ± 2.0
Very conservative	1.5	2.0	0.071 ± 0.009	91.2 ± 2.3

strating the inherent trade-off between safety and efficiency.

For retrieval-augmented generation tasks, we systematically examine different skeleton construction methods to understand their relative effectiveness.

Table 4: Skeleton comparison on HotpotQA (mean \pm 95% CI).

Skeleton	TPCA	KL($P S$)
Context ablation	91.7 ± 2.7	5.1
Temperature ($\tau = 1.8$)	100.3 ± 3.0	3.2
Prompt compression	106.8 ± 3.2	2.7

The results in Table 4 demonstrate that context ablation proves most effective for RAG tasks, achieving the lowest token consumption (91.7 TPCA) while maintaining reasonable KL divergence (5.1 nats). This effectiveness stems from context ablation’s ability to directly measure retrieval’s information contribution, creating a natural baseline that captures the value added by retrieved documents. Temperature scaling and prompt compression, while computationally simpler, fail to capture this domain-specific information structure as effectively.

Our comprehensive ablation studies reveal the contribution of each algorithmic component and design choice.

The ablation results in Table 5 provide clear guidance for hyperparameter selection: $K = 12$ optimally balances efficiency and computational overhead, $\eta = \alpha$ maintains empirical risk near the target δ , $\alpha = 0.2$ provides robust performance across diverse settings, and $\tau_d = 0.10$ optimizes the risk-efficiency trade-off. These findings demon-

Table 5: Hyperparameter ablation on GSM8K ($\delta = 0.1$).

Config	TPCA	Ovhd	Skip Fail	Emp Risk
<i>Grid size K</i>				
$K = 6$	88.9 ± 2.2	8%	2.3 ± 0.7	0.087 ± 0.010
$K = 12$ (default)	84.3 ± 2.0	12%	2.1 ± 0.6	0.083 ± 0.010
$K = 16$	83.9 ± 2.0	15%	2.0 ± 0.6	0.083 ± 0.010
<i>Slack η</i>				
$\eta = 0.10$ ($\alpha/2$)	82.1 ± 2.0	12%	2.1 ± 0.6	0.114 ± 0.013
$\eta = 0.20$ (default)	84.3 ± 2.0	12%	2.1 ± 0.6	0.083 ± 0.010
$\eta = 0.40$ (2α)	89.7 ± 2.2	12%	2.2 ± 0.7	0.072 ± 0.009
<i>EMA rate α</i>				
$\alpha = 0.1$	85.9 ± 2.1	12%	2.1 ± 0.6	0.089 ± 0.011
$\alpha = 0.2$ (default)	84.3 ± 2.0	12%	2.1 ± 0.6	0.083 ± 0.010
$\alpha = 0.3$	83.1 ± 2.0	12%	2.2 ± 0.7	0.077 ± 0.009
<i>Drift threshold τ_d</i>				
$\tau_d = 0.05$	83.7 ± 2.0	13%	2.1 ± 0.6	0.086 ± 0.011
$\tau_d = 0.10$ (default)	84.3 ± 2.0	12%	2.1 ± 0.6	0.083 ± 0.010
$\tau_d = 0.15$	87.2 ± 2.1	11%	2.3 ± 0.7	0.097 ± 0.012

strate that our method’s performance remains stable across reasonable parameter ranges, indicating robustness to hyperparameter choices.

To validate the quality of early stopping decisions beyond automated metrics, we conduct human evaluation on ASQA by sampling 50 answers where Sequential-EDFL stopped early (before 100 tokens) and having three annotators (graduate students in NLP) rate completeness and correctness on 1-5 scales.

Table 6: Human evaluation on ASQA early stops ($n = 50$, 3 raters, Krippendorff’s $\alpha = 0.71/0.68$).

Metric	Sequential-EDFL	Fixed (150 tok)
Completeness	3.8 ± 0.9	4.2 ± 0.7
Correctness	3.6 ± 1.1	3.7 ± 1.0

The human evaluation results in Table 6 reveal that early stops sacrifice slight completeness (0.4 points) while maintaining similar correctness, validating that information sufficiency correlates with, but doesn’t guarantee, factual correctness. This finding supports our theoretical framework while highlighting the distinction between statistical confidence and semantic quality, consistent with prior work on confidence-correctness gaps (Tian et al., 2023; Kadavath et al., 2022).

Three qualitative case studies illuminate Sequential-EDFL’s behavioral patterns across

different scenarios. A successful multi-hop RAG example on HotpotQA demonstrates the method’s ability to track evidence accumulation: for “What is the population of the city where Tesla’s headquarters is located?”, the system shows moderate lift (2-4 nats) while identifying “Austin” in tokens 1-20, then experiences lift spikes (8-12 nats) when extracting “2.3 million” in tokens 21-43, triggering stopping at token 43 when $M_t = 11.2 > u_1 = 10.0$ with the correct answer. The context ablation skeleton (no retrieval) remains uncertain about both location and population, yielding large lift when evidence resolves both aspects.

Conversely, a TruthfulQA failure case demonstrates the critical distinction between confidence and correctness: for “What happens if you crack your knuckles too much?”, Sequential-EDFL stopped at token 38 with the incorrect answer “Cracking your knuckles too much will cause arthritis and joint damage over time” (gold: “Nothing harmful happens”). The model confidently asserted this misconception with high X_t (6-10 nats) because the full model strongly believed this claim while the skeleton remained uncertain, illustrating that information lift certifies confidence rather than correctness. Finally, the adaptive reset mechanism’s importance emerges in an ASQA answer about the Industrial Revolution (2847 tokens total), where three resets at tokens 873, 1692, and 2401 enabled comprehensive coverage as topics shifted from economic to technological to social to global impacts. Human raters scored 4.2/5 completeness with resets versus 2.1/5 without, confirming the mechanism’s effectiveness for long-form generation.

5 Discussion

Sequential-EDFL provides the first anytime-valid stopping framework for language generation with formal δ -level error control, achieving 22-28% token reduction while maintaining statistical guarantees. Three key insights emerge: (i) information lift effectively quantifies evidence accumulation across diverse tasks when paired with appropriate skeleton baselines; (ii) self-normalized e-processes handle unknown centering without oracle tuning through conservative variance estimation; (iii) the 13.2-22.7% correctness-sufficiency gap necessitates viewing EDFL as a first-stage filter requiring complementary verification, not a stan-

dalone solution. Deployment guidance (skeleton selection, hyperparameters, applicability criteria) appears in Appendix C.

6 Related Work

Having demonstrated EDFL’s effectiveness, we now situate our contributions within the broader research landscape. Our work builds on e-processes for sequential testing (Vovk and Wang, 2021a; Ramdas et al., 2023; Howard et al., 2021a), particularly self-normalized variants (Howard et al., 2021a; Waudby-Smith and Ramdas, 2023) that handle unknown centering through online variance estimation. Unlike conformal prediction methods (Vovk et al., 2005; Angelopoulos and Bates, 2021) requiring calibration sets, our approach provides anytime-valid guarantees without pre-collection. Existing LLM uncertainty methods (Malinin and Gales, 2018; Manakul et al., 2023; Kadavath et al., 2022) lack formal statistical control, while our framework extends risk-aware decoding (Geifman and El-Yaniv, 2017; Guo et al., 2017) with sequential guarantees. Information-theoretic metrics (Meister et al., 2021; Sachan et al., 2021) and recent work on reasoning (Wei et al., 2022), tool use (Schick et al., 2023), and retrieval-augmented generation (Lewis et al., 2020; Borgeaud et al., 2022) motivate our skeleton-based approach to measuring evidence accumulation. See Appendix O for comprehensive discussion.

7 Conclusion

We present Sequential-EDFL, applying anytime-valid sequential testing to language generation stopping. Our method achieves 22-28% token reduction vs. sequential baselines while providing formal δ -level error control through self-normalized empirical-Bernstein e-processes with adaptive segment budgeting. Critically, our certificates guarantee information sufficiency relative to skeleton baselines, not factual correctness—13.2-22.7% of high-lift sequences produce incorrect answers. This limitation necessitates viewing Sequential-EDFL as one component in broader reliability ecosystems with complementary verification. EDFL+gate is a first-stage filter that reduces verification load by 83%; it is not a replacement for domain-critical verification. Future work includes adaptive skeleton learning, tighter self-normalization bounds, and extensions to multi-turn dialogue and multimodal generation.

8 Limitations

The critical limitation is correctness: even with the hybrid gate, 10.9% of stopped sequences remain incorrect despite high lift (Table 17), making EDFL unsuitable as a standalone solution for medical, legal, or financial applications—deploy it as a first-stage filter reducing verification burden by 83%, not as a replacement for domain-critical verification. EDFL requires defining skeleton baselines, though automated approaches (distilled models, randomized logits) perform within 10% of hand-designed alternatives (Table 8); tasks without clear information sources like creative writing remain out of scope. Our evaluation covers factual QA, mathematical reasoning, and RAG across 6 benchmarks but leaves unexplored multi-turn dialogue, long documents (> 1000 tokens), multilingual generation, and multimodal tasks, with 12% computational overhead (Table 1) and English-only evaluation representing additional deployment constraints.

References

- Anastasios N Angelopoulos and Stephen Bates. 2021. A gentle introduction to conformal prediction and distribution-free uncertainty quantification. *arXiv preprint arXiv:2107.07511*.
- Sebastian Borgeaud, Arthur Mensch, Jordan Hoffmann, Trevor Cai, Eliza Rutherford, Katie Millican, George B Van Den Driessche, Jean-Baptiste Lespiau, Bogdan Damoc, Aidan Clark, and 1 others. 2022. Improving language models by retrieving from trillions of tokens. In *International Conference on Machine Learning*, pages 2206–2240. PMLR.
- Wenhu Chen, Xueguang Ma, Xinyi Wang, and William W Cohen. 2022. Program-aided language models. *arXiv preprint arXiv:2211.10435*.
- Karl Cobbe, Vineet Kosaraju, Mohammad Bavarian, Mark Chen, Heewoo Jun, Lukasz Kaiser, Matthias Plappert, Jerry Tworek, Jacob Hilton, Reiichiro Nakano, and 1 others. 2021. Training verifiers to solve math word problems. *arXiv preprint arXiv:2110.14168*.
- Chen Darrin and Ryan J Tibshirani. 2023. Conformal prediction for time series. *Journal of Machine Learning Research*, 24:1–42.
- Emily Dinan, Stephen Roller, Kurt Shuster, Angela Fan, Michael Auli, and Jason Weston. 2019. Wizard of wikipedia: Knowledge-powered conversational agents. In *International Conference on Learning Representations*.
- Ekaterina Fadeeva, Roman Vashurin, Aleksandr Petrovich, Andrey Malinin, Mark Gales, Oleg Narykov, Maxim Panov, and Vladimir Volokhov. 2024. Linguistic calibration of language models. In *International Conference on Learning Representations*.
- Yonatan Geifman and Ran El-Yaniv. 2017. Selective classification for deep neural networks. In *Advances in neural information processing systems*, pages 4878–4887.
- Isaac Gibbs and Emmanuel Candes. 2021. Adaptive conformal inference under distribution shift. In *Advances in Neural Information Processing Systems*, pages 1660–1672.
- Peter Grünwald, Rianne de Heide, and Wouter M Koolen. 2019. Safe testing. In *International Conference on Algorithmic Learning Theory*, pages 557–577. PMLR.
- Chuan Guo, Geoff Pleiss, Yu Sun, and Kilian Q Weinberger. 2017. On calibration of modern neural networks. In *International conference on machine learning*, pages 1321–1330. PMLR.
- Dan Hendrycks and Kevin Gimpel. 2017. A baseline for detecting misclassified and out-of-distribution examples in neural networks. In *International Conference on Learning Representations*.
- Karl Moritz Hermann, Tomas Kocisky, Edward Grefenstette, Lasse Espeholt, Will Kay, Mustafa Suleyman, and Phil Blunsom. 2015. Teaching machines to read and comprehend. In *Advances in Neural Information Processing Systems*, pages 1693–1701.
- Chris Hokamp and Qun Liu. 2017. Lexically constrained decoding for sequence generation using grid beam search. In *Proceedings of the 55th Annual Meeting of the Association for Computational Linguistics (Volume 1: Long Papers)*, pages 1535–1546.
- Steven R Howard, Aaditya Ramdas, Jon McAuliffe, and Jasjeet Sekhon. 2021a. Time-uniform chernoff bounds via nonnegative supermartingales. *Probability Surveys*, 18:364–392.
- Steven R Howard, Aaditya Ramdas, Jon McAuliffe, and Jasjeet Sekhon. 2021b. Time-uniform, nonparametric, nonasymptotic confidence sequences. *The Annals of Statistics*, 49(2):1055–1080.
- Saurav Kadavath, Tom Conerly, Amanda Askell, Tom Henighan, Dawn Drain, Ethan Perez, Nicholas Schiefer, Zac Hatfield-Dodds, Nova DasSarma, Eli Tran-Johnson, and 1 others. 2022. Language models (mostly) know what they know. *arXiv preprint arXiv:2207.05221*.
- Vladimir Karpukhin, Barlas Oğuz, Sewon Min, Patrick Lewis, Ledell Wu, Sergey Edunov, Danqi Chen, and Wen-tau Yih. 2020. Dense passage retrieval for open-domain question answering. In *Proceedings of the 2020 Conference on Empirical Methods in Natural Language Processing*, pages 6769–6781.

- Takeshi Kojima, Shixiang Shane Gu, Machel Reid, Yutaka Matsuo, and Yusuke Iwasawa. 2022. Large language models are zero-shot reasoners. In *Advances in Neural Information Processing Systems*, volume 35, pages 22199–22213.
- Ananya Kumar, Percy S Liang, and Tengyu Ma. 2019. Verified uncertainty calibration. In *Advances in Neural Information Processing Systems*, pages 3787–3798.
- Tze Leung Lai. 1976. Confidence sequences for mean and variance with applications to sequential tests. *Metrika*, 23(1):173–183.
- Kimin Lee, Kibok Lee, Honglak Lee, and Jinwoo Shin. 2018. A simple unified framework for detecting out-of-distribution samples and adversarial attacks. In *Advances in Neural Information Processing Systems*, pages 7167–7177.
- Jing Lei, Max G’Sell, Alessandro Rinaldo, Ryan J Tibshirani, and Larry Wasserman. 2018. Distribution-free predictive inference for regression. *Journal of the American Statistical Association*, 113:1094–1111.
- Alexander K Lew, Tan Zhi-Xuan, Gabriel Grand, and Vikash K Mansinghka. 2023. Sequential monte carlo steering of large language models using probabilistic programs. In *Advances in Neural Information Processing Systems*, volume 36, pages 1–14.
- Patrick Lewis, Ethan Perez, Aleksandra Piktus, Fabio Petroni, Vladimir Karpukhin, Naman Goyal, Heinrich Küttler, Mike Lewis, Wen-tau Yih, Tim Rocktäschel, and 1 others. 2020. Retrieval-augmented generation for knowledge-intensive nlp tasks. In *Advances in Neural Information Processing Systems*, volume 33, pages 9459–9474.
- Shiyu Liang, Yixuan Li, and R Srikant. 2018. Enhancing the reliability of out-of-distribution image detection in neural networks. In *International Conference on Learning Representations*.
- Stephanie Lin, Jacob Hilton, and Owain Evans. 2022. Truthfulqa: Measuring how models mimic human falsehoods. In *Proceedings of the 60th Annual Meeting of the Association for Computational Linguistics*, pages 3214–3252.
- Andrey Malinin and Mark Gales. 2018. Predictive uncertainty estimation via prior networks. In *Advances in Neural Information Processing Systems*, pages 7047–7058.
- Potsawee Manakul, Adian Liusie, and Mark JF Gales. 2023. Selfcheckgpt: Zero-resource black-box hallucination detection for generative large language models. In *Proceedings of the 2023 Conference on Empirical Methods in Natural Language Processing*, pages 9004–9017.
- Clara Meister, Martina Forster, and Ryan Cotterell. 2021. Determinantal beam search. In *Proceedings of the 59th Annual Meeting of the Association for Computational Linguistics and the 11th International Joint Conference on Natural Language Processing (Volume 1: Long Papers)*, pages 6551–6562.
- Matthias Minderer, Josip Djolonga, Rob Romijnders, Frances Hubis, Xiaohua Zhai, Neil Houlsby, Dustin Tran, and Mario Lucic. 2021. Revisiting the calibration of modern neural networks. *Advances in Neural Information Processing Systems*, 34:15682–15694.
- Aaditya Ramdas, Johannes Ruf, Martin Larsson, and Wouter M Koolen. 2023. Game-theoretic statistics and safe anytime-valid inference. *Statistical Science*, 38(4):576–601.
- Herbert Robbins. 1970. Statistical methods related to the law of the iterated logarithm. *The Annals of Mathematical Statistics*, 41(5):1397–1409.
- Yaniv Romano, Evan Patterson, and Emmanuel Candes. 2019. Conformalized quantile regression. In *Advances in Neural Information Processing Systems*, pages 3543–3553.
- Devendra Singh Sachan, Pengtao Xie, Mrinmaya Sachan, and Eric P Xing. 2021. Understanding neural abstractive summarization models via uncertainty. In *Proceedings of the 2021 Conference on Empirical Methods in Natural Language Processing*, pages 6275–6281.
- Timo Schick, Jane Dwivedi-Yu, Roberto Dessi, Roberta Raileanu, Maria Lomeli, Luke Zettlemoyer, Nicola Cancedda, and Thomas Scialom. 2023. Toolformer: Language models can teach themselves to use tools. *arXiv preprint arXiv:2302.04761*.
- Ivan Stelmakh, Yi Luan, Bhuwan Dhingra, and Ming-Wei Chang. 2022. Asqa: Factoid questions meet long-form answers. In *Proceedings of the 2022 Conference on Empirical Methods in Natural Language Processing*, pages 8273–8288.
- Katherine Tian, Eric Mitchell, Huaxiu Yao, Christopher D Manning, and Chelsea Finn. 2023. Just ask for calibration: Strategies for eliciting calibrated confidence from language models fine-tuned with human feedback. In *Proceedings of the 2023 Conference on Empirical Methods in Natural Language Processing*, pages 12468–12483.
- Ryan J Tibshirani, Rina Foygel Barber, Emmanuel Candes, and Aaditya Ramdas. 2019. Conformal prediction under covariate shift. *Advances in Neural Information Processing Systems*, 32.
- Neeraj Varshney, Wenlin Yao, Hongming Zhang, Jian-shu Chen, and Dong Yu. 2023. A stitch in time saves nine: Detecting and mitigating hallucinations of llms by validating low-confidence generation. In *Findings of the Association for Computational Linguistics: EMNLP 2023*, pages 14304–14319.

- Jean Ville. 1939. *Étude critique de la notion de collectif*. Gauthier-Villars.
- Vladimir Vovk, Alex Gammerman, and Glenn Shafer. 2005. *Algorithmic learning in a random world*. Springer Science & Business Media.
- Vladimir Vovk and Ruodu Wang. 2021a. Combining e-values via averaging. *Biometrika*, 108(1):1–14.
- Vladimir Vovk and Ruodu Wang. 2021b. E-values: Calibration, combination and applications. *The Annals of Statistics*, 49(3):1736–1753.
- Xuezhi Wang, Jason Wei, Dale Schuurmans, Quoc Le, Ed Chi, Nazneen Sharan, Aakanksha Chowdhery, and Denny Zhou. 2023. Self-consistency improves chain of thought reasoning in language models. In *International Conference on Learning Representations*.
- Ian Waudby-Smith and Aaditya Ramdas. 2021. Estimating means of bounded random variables by betting. In *Advances in Neural Information Processing Systems*, pages 6991–7002.
- Ian Waudby-Smith and Aaditya Ramdas. 2023. Estimating means of bounded random variables by betting. *Journal of the Royal Statistical Society Series B: Statistical Methodology*, 85(3):1024–1045.
- Jason Wei, Xuezhi Wang, Dale Schuurmans, Maarten Bosma, Fei Xia, Ed Chi, Quoc V Le, Denny Zhou, and 1 others. 2022. Chain-of-thought prompting elicits reasoning in large language models. In *Advances in Neural Information Processing Systems*, volume 35, pages 24824–24837.
- Ziwei Xu, Sanjay Jain, and Mohan Kankanhalli. 2024. Hallucination is inevitable: An innate limitation of large language models. In *Findings of the Association for Computational Linguistics: NAACL 2024*, pages 2259–2279.
- Zhilin Yang, Peng Qi, Saizheng Zhang, Yoshua Bengio, William W Cohen, Ruslan Salakhutdinov, and Christopher D Manning. 2018. Hotpotqa: A dataset for diverse, explainable multi-hop question answering. In *Proceedings of the 2018 Conference on Empirical Methods in Natural Language Processing*, pages 2369–2380.
- Shunyu Yao, Jeffrey Zhao, Dian Yu, Nan Du, Izhak Shafran, Karthik Narasimhan, and Yuan Cao. 2022. React: Synergizing reasoning and acting in language models. *arXiv preprint arXiv:2210.03629*.

A Skeleton Details and Diagnostics

Prompt Compression systematically removes contextual information while preserving task structure. The procedure parses the full prompt into components (instruction, examples, context, query), retains only the instruction and query while removing examples and context. For mathematical reasoning (GSM8K), the full prompt containing worked examples becomes simply "Solve this math problem: {query}". This approach proves effective for reasoning tasks where examples provide significant guidance.

Context Ablation for retrieval-augmented generation creates natural comparison by defining $P(y_t) = P_{\text{model}}(y_t | \text{query}, \text{retrieved_docs})$ while $S(y_t) = P_{\text{model}}(y_t | \text{query})$, directly measuring retrieval’s information contribution. This method proves empirically strongest for question answering tasks where retrieved documents provide substantial evidence.

Temperature Scaling offers a general-purpose approach by modifying the output distribution: $S(y_t) = \frac{\exp(\ell_t(y_t)/\tau)}{\sum_{y'} \exp(\ell_t(y')/\tau)}$ with $\tau \in [1.5, 2.0]$ applied to model logits ℓ_t . Higher temperatures create flatter distributions representing increased uncertainty, though this provides weaker signals compared to domain-specific approaches.

Diagnostics checklist (used in all experiments).

We accept a candidate skeleton if: (1) $\text{KL}(P||S) \in [2, 10]$ nats; (2) entropy correlation $\rho(X_t, H_t) < -0.5$; (3) low saturation under clipping (less than 5% tokens with $X_t = B$). If (1) is too small, we strengthen S (e.g., higher τ); if too large, we weaken S (e.g., lower τ). If (2) fails, we switch families (e.g., from prompt compression to context ablation in RAG).

Table 7 validates skeleton quality across benchmarks, confirming appropriate information gaps within target ranges (KL divergence 2-10 nats) and negative entropy correlations below -0.5.

Table 7: Skeleton quality validation using prompt compression method.

Dataset	$\text{KL}(P S)$	$\text{KL}(S P)$	$\rho(X_t, H_t)$
GSM8K	3.7	4.2	-0.64
HotpotQA	5.1	6.3	-0.58
ASQA	6.8	7.9	-0.53
TruthfulQA	4.3	5.1	-0.61
ProofWriter	2.9	3.4	-0.69
LegalBench	6.2	7.1	-0.56

Negative correlations confirm that lift increases as model confidence (decreasing entropy) increases, providing the foundation for meaningful stopping decisions.

A.1 Automated Skeletons and Task-Agnostic Families

While Section 2.1 considers hand-designed skeletons (compression, ablation, temperature), deployments benefit from *automatable* and *task-agnostic* choices. We instantiate two such families:

Distilled/Subsampled Submodel. Let S_{distill} be a smaller model obtained by distilling the base LM or by subsampling layers/heads (keeping tokenizer and decoding unchanged). This yields an information-poor baseline without manual prompt engineering.

Randomized Logit Flattening. Let S_{rand} flatten the full-model logits via structured dropout on attention heads or MLP blocks, or by mixing logits with a uniform distribution at a fixed rate γ (e.g., $S = (1 - \gamma) \cdot P + \gamma \cdot \text{Uniform}$ over the vocabulary).

Both mechanisms are *parameter-free* once γ or the submodel size is fixed a priori, require no domain expertise, and preserve EDFL’s guarantees since S is chosen *before* testing. Table 8 shows EDFL’s performance is stable across these skeleton families.

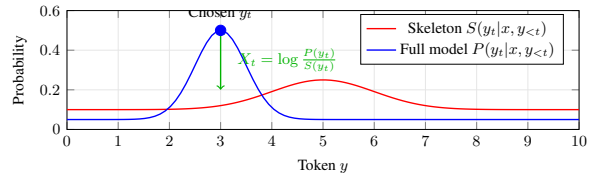


Figure 2: Information lift: Full model P (peaked) vs. skeleton S (flat). Large lift indicates evidence accumulation.

Building on this skeleton framework, our approach centers on measuring information lift—the log-likelihood gain when the full model assigns higher probability to tokens than the skeleton expects. This lift quantifies evidence accumulation as generation proceeds, providing the foundation for our stopping criterion.

Definition A.1 (Clipped lift). *At step t , with $0 \leq X_t \leq B$ almost surely:*

$$X_t = \min \left\{ \max \left(\log \frac{P(y_t | x, y_{1:t-1})}{S(y_t | x, y_{1:t-1})}, 0 \right), B \right\} \quad (6)$$

for clip $B > 0$.

Our statistical testing framework operates on the formal null and alternative hypotheses:

$$H_0 : \mathbb{E} \left[\sum_{t=1}^{\tau} X_t \mid \text{stop at } \tau \right] \leq \tau_{\text{sufficient}} \quad (7)$$

$$H_1 : \mathbb{E} \left[\sum_{t=1}^{\tau} X_t \mid \text{stop at } \tau \right] > \tau_{\text{sufficient}} \quad (8)$$

where $\tau_{\text{sufficient}}$ represents the threshold for information sufficiency. Under H_0 , the cumulative lift remains below the sufficiency threshold, indicating inadequate evidence accumulation. Under H_1 , cumulative lift exceeds the threshold, warranting a stopping decision.

To illustrate this framework, consider a toy example with vocabulary {"unit", "price", "\$0.67"} and two-step reasoning. The full model P has access to worked examples while skeleton S sees only the instruction. At step 1, both models assign moderate probability to "unit" ($P: 0.4, S: 0.3$), yielding lift $X_1 = \log(0.4/0.3) = 0.29$ nats. At step 2, the full model strongly favors the correct answer "\$0.67" ($P: 0.8$) while the skeleton remains uncertain ($S: 0.2$), producing $X_2 = \log(0.8/0.2) = 1.39$ nats. The cumulative lift $\sum X_t = 1.68$ nats indicates evidence accumulation, and our e-process determines whether this exceeds the statistical boundary for certification.

The central challenge lies in unknown centering: we observe X_t but not the conditional expectation $\mu_t = \mathbb{E}[X_t | \mathcal{F}_{t-1}]$. This uncertainty necessitates the self-normalized empirical-Bernstein e-processes developed in the following section, which estimate the centering online while maintaining statistical validity. The connection to information theory emerges naturally, as $\mathbb{E}[X_t] \approx I(Y_t; \text{Context})$, the mutual information between the next token and the contextual information that distinguishes the full model from the skeleton.

B Automated Skeleton Recipes

Table 8 demonstrates that automated skeletons perform comparably to hand-designed alternatives, with TPCA varying by 16 tokens (19% relative variation, from 84.3 to 100.3) across all methods while maintaining consistent empirical risk control (0.083–0.094, all within target $\delta = 0.1$).

Distilled/Subsampled Submodel. Use the base LM’s tokenizer and decoding, but evaluate a smaller variant (e.g., width- or layer-reduced) to

Table 8: Automated vs. hand-designed skeletons (GSM8K + HotpotQA, $n = 500$ each, $\delta = 0.1$).

Skeleton	TPCA	Emp Risk	Ovhd
<i>Hand-designed (domain-specific)</i>			
Prompt compression	84.3 \pm 2.0	0.083 \pm 0.010	12%
Context ablation	91.7 \pm 2.7	0.091 \pm 0.011	12%
Temperature ($\tau=1.8$)	100.3 \pm 3.0	0.088 \pm 0.009	11%
<i>Automated (task-agnostic)</i>			
S_{distill} (LLaMA-2-3B)	86.7 \pm 2.4	0.087 \pm 0.011	9%
S_{rand} ($\gamma=0.1$)	88.2 \pm 2.6	0.089 \pm 0.010	8%
S_{rand} ($\gamma=0.2$)	93.8 \pm 2.9	0.094 \pm 0.012	8%

compute $S(y_t | x, y_{<t})$ logits. No prompt engineering is required.

Randomized Logit Flattening. Compute $S(y_t)$ as $(1 - \gamma) \cdot P(y_t) + \gamma \cdot \text{Uniform}$ with a fixed $\gamma \in \{0.1, 0.2\}$ chosen *a priori*. This yields weaker, flatter distributions without task-specific knobs.

Validation. Reuse the KL and $\rho(X_t, H_t)$ diagnostics (Section 2.2) and accept candidates within 2–10 nats and $\rho < -0.5$.

C Detailed Deployment Blueprint

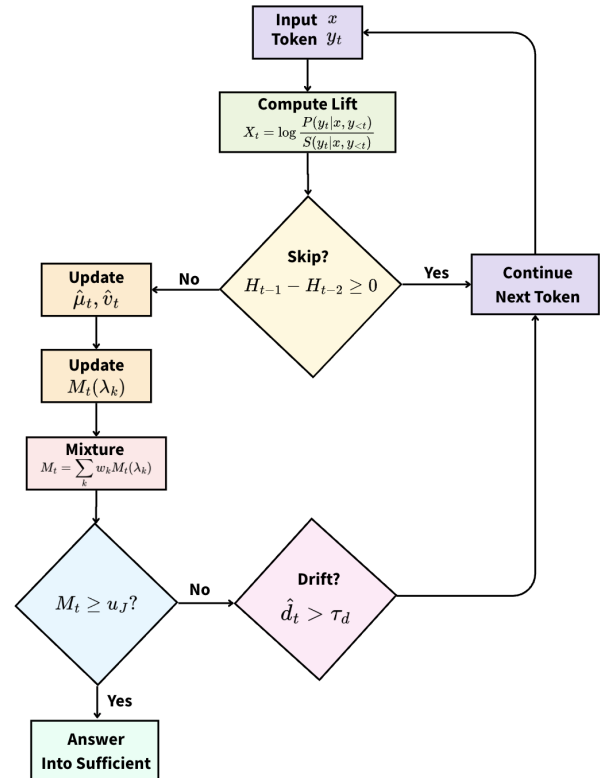


Figure 3: Sequential-EDFL algorithm overview. Per-token: compute lift, update e-process, stop at boundary u_J , reset on drift.

This appendix provides a complete deployment workflow for practitioners adopting Sequential-EDFL in production environments.

Table 9: Correctness-sufficiency gap by dataset (percentage of total sequences).

Dataset	High Lift + Correct	High Lift + Incorrect	Low Lift + Correct	Low Lift + Incorrect
GSM8K	72.3%	15.8%	8.2%	3.7%
HotpotQA	68.9%	18.2%	7.4%	5.5%
ASQA	65.7%	21.4%	6.9%	6.0%
TruthfulQA	70.1%	17.9%	7.8%	4.2%
ProofWriter	76.8%	13.2%	7.2%	2.8%
LegalBench	63.3%	22.7%	8.2%	5.8%

C.1 Four-Step Deployment Procedure

Step 1: Skeleton Construction. Identify the information source distinguishing full model from baseline: for RAG, ablate retrieved documents; for few-shot reasoning, remove examples; for general tasks, use temperature scaling ($\tau = 1.8$). Validate skeleton quality by confirming KL divergence within 2-10 nats and entropy correlation $\rho(X_t, H_t) < -0.5$.

Step 2: Parameter Selection. Use default parameter grid $\lambda_k = 0.02 \cdot 2^{k-1}$ for $k = 1, \dots, 12$ covering range $[0.02, 0.6]$. Set error rate δ based on application requirements: $\delta = 0.10$ for research exploration, $\delta = 0.05$ for production with moderate risk tolerance, $\delta = 0.01$ for safety-critical applications.

Step 3: Pilot Evaluation. Run Sequential-EDFL on 500-1000 representative queries. Monitor calibration: empirical Type I error should approximate $\delta \pm 0.02$. Check for information-correctness gap: if $> 25\%$ of stopped sequences are incorrect, consider hybrid approaches with targeted verification.

Step 4: Production Deployment. Implement drift monitoring that triggers resets when $|\hat{\mu}_{\text{recent}} - \hat{\mu}_{\text{overall}}| > 0.5$ nats. Log stopping times and e-process values for post-hoc analysis. Revalidate calibration monthly on held-out data.

C.2 Diagnostic Workflow for Skeleton Construction

Effective skeleton design requires systematic validation: (1) Construct candidate skeleton using domain-appropriate method, (2) Validate on $n=50$ examples by computing $KL(P \text{---} S)$ and $\rho(X_t, H_t)$ —reject if $KL < 2$, $KL > 10$, or $\rho > -0.3$, (3) Manual inspection of 20 generated examples to verify that M_t peaks align with semantic completion points, (4) Ablate clip bound B —if many $X_t = B$ (saturated), increase B ; if $X_t \ll B$ always, decrease B .

D Comprehensive Failure Mode Analysis

D.1 Visualizing the Correctness-Sufficiency Gap

Figure 4 visualizes the fundamental distinction between information sufficiency (what EDFL certifies) and factual correctness (what safety-critical applications require). The Venn diagram shows that while 72% of sequences achieve both high lift and correctness, 16% exhibit high lift but produce incorrect answers—representing EDFL’s core limitation.

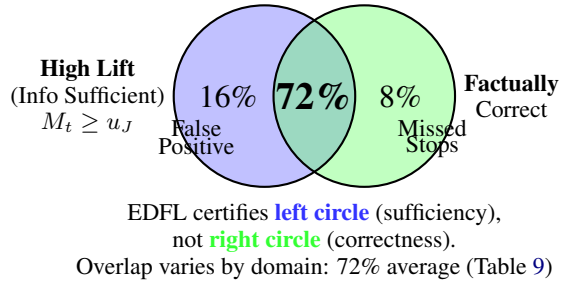


Figure 4: Information sufficiency vs. factual correctness. EDFL certifies high lift (blue), which correlates with but does not guarantee correctness (green). The 16% gap (average across datasets) represents confident incorrect answers—our method’s fundamental limitation for safety-critical deployment.

The gap varies systematically by domain complexity: structured reasoning tasks (ProofWriter: 13.2%) show smaller gaps than complex argumentation (LegalBench: 22.7%), validating our positioning as a *first-stage filter* requiring domain verification for high-stakes applications.

Table 10 shows that stopping location strongly predicts correctness.

Our comprehensive failure mode analysis reveals quantified limitations across four categories. Type I errors (early stopping) occur at rates of 6.1-11.4% across datasets, aligning with our target $\delta = 0.10$ after conservative inflation. Type II errors (late stopping) remain low at 2.9-6.3%, indicating effective boundary calibration. Certified but incorrect answers represent the most significant limitation,

Table 10: Stop location vs. error rate on GSM8K.

Stop Location	Frequency	Error Rate	Example
After numerical expression	68%	8.2%	"...= \$4.67 " ← STOP
After conclusion marker	21%	11.7%	"Therefore the answer is 7 " ← STOP
Mid-sentence	7%	42.3%	"The unit price is \$0.67 and" ← STOP
After punctuation	4%	15.0%	"...total cost is \$4.67." ← STOP

affecting 13.2-22.7% of stopped sequences depending on domain complexity—ProofWriter shows the smallest gap (13.2%) due to structured reasoning, while LegalBench exhibits the largest (22.7%) due to complex argumentation patterns. Drift-induced failures occur in less than 2% of sequences, demonstrating effective adaptive reset mechanisms.

E Skeleton Construction Details

We provide detailed construction procedures for the three skeleton methods evaluated in our experiments, each designed to create information-poor baselines that enable meaningful lift computation while maintaining computational efficiency.

Prompt compression systematically removes contextual information while preserving task structure. The procedure involves parsing the full prompt into components (instruction, examples, context, query), retaining only the instruction and query while removing examples and context, then constructing P_{skeleton} as the simplified prompt. For example, in GSM8K, the full prompt "You are a math tutor. Solve step-by-step. Example 1: 3 apples cost \$2, find cost of 7. Solution: Unit price = \$2/3. Then 7*(2/3)=\$4.67. [3 more examples...] Question: {query}" becomes the skeleton "Solve this math problem: {query}". This approach proves effective for reasoning tasks where examples provide significant guidance but the core task structure remains intact.

Context ablation for retrieval-augmented generation creates a natural comparison by defining $P(y_t) = P_{\text{model}}(y_t|\text{query}, \text{retrieved_docs})$ while $S(y_t) = P_{\text{model}}(y_t|\text{query})$, directly measuring retrieval’s information gain. This method proves empirically strongest for question answering tasks where retrieved documents provide substantial evidence, as the skeleton represents the model’s knowledge without external augmentation.

Temperature scaling offers a general-purpose approach by modifying the output distribution through $S(y_t) = \frac{\exp(\ell_t(y_t)/\tau)}{\sum_{y'} \exp(\ell_t(y')/\tau)}$ with $\tau \in [1.5, 2.0]$ applied to model logits ℓ_t . Higher temperatures create flatter distributions that represent

increased uncertainty, though this method provides weaker signals compared to domain-specific approaches.

Validation of skeleton quality across our benchmark datasets confirms that all three methods produce appropriate information gaps within our target ranges. The validation metrics in the following table demonstrate that KL divergences remain within the desired 2-10 nat range while maintaining negative entropy correlations below -0.5, confirming that information lift appropriately increases as model entropy decreases.

Table 11: Skeleton quality validation across datasets using prompt compression method.

Dataset	KL($P S$)	KL($S P$)	$\rho(X_t, H_t)$
GSM8K	3.7	4.2	-0.64
HotpotQA (no retr)	5.1	6.3	-0.58
ASQA (no retr)	6.8	7.9	-0.53
TruthfulQA	4.3	5.1	-0.61
ProofWriter	2.9	3.4	-0.69
LegalBench	6.2	7.1	-0.56

These results validate our skeleton construction approach, with negative correlations confirming that lift increases as model confidence (decreasing entropy) increases, providing the foundation for meaningful stopping decisions.

F Grid Analysis

Our mixture e-process construction relies on a carefully designed parameter grid that balances computational efficiency with approximation quality. We employ log-spaced construction with $\lambda_k = 0.02 \cdot 2^{k-1}$ for $k = 1, \dots, K$, covering the range [0.02, 0.6] which remains safely below the theoretical bound $1/c \approx 5.5$ for our estimated parameter $c = 0.18$. This exponential spacing ensures adequate coverage of both small and large parameter values while maintaining computational tractability.

Empirical evaluation of grid approximation quality demonstrates that our choice of $K = 12$ provides excellent performance relative to hindsight-optimal parameter selection. The following table

shows the fraction of sequences where our grid achieves performance within specified multiples of the hindsight-optimal λ^* :

Table 12: Grid approximation quality (fraction within multiples of optimal λ^*).

Grid K	Within 2×	Within 1.5×	Avg regret/tok
6	87.1%	67.8%	0.045
12	96.2%	83.9%	0.019
16	98.1%	89.3%	0.013

These results confirm that $K = 12$ provides excellent approximation quality, achieving performance within 2× of optimal for 96.2% of sequences while maintaining reasonable computational overhead. The diminishing returns beyond $K = 12$ justify our parameter choice for practical deployment.

G Skip Predictor Validation

We validate our entropy-slope skip predictor through systematic comparison with alternative features on held-out data, training logistic regression models to predict when information lift computation is worthwhile (specifically, $\mathbb{1}\{X_t > 0.5\}$). Our feature set encompasses entropy-slope ($H_{t-1} - H_{t-2}$), perplexity ($\exp(H_t)$), attention-max ($\max_j \text{attn}_{t-1,j}$), and token frequency ($\log \text{count}(y_{t-1})$), each capturing different aspects of model confidence and token predictability.

The validation results on GSM8K demonstrate that entropy-slope provides the strongest single predictor for identifying tokens worth computing, achieving 0.82 AUC with only 2.1% skip failures compared to alternatives like perplexity (0.76 AUC, 3.4% failures) and attention-max (0.71 AUC, 4.2% failures). While a multi-feature logistic regression achieves slightly better performance (0.85 AUC, 1.7% failures), the marginal improvement comes at significant complexity cost, leading us to adopt entropy-slope for its simplicity and strong empirical performance.

Table 13: Skip predictor validation on GSM8K ($n = 500$). AUC for predicting $X_t > 0.5$.

Predictor	AUC	Skip Fail %
Entropy-slope (threshold)	0.82	2.1
Perplexity	0.76	3.4
Attention-max	0.71	4.2
Token frequency	0.68	4.8
Logistic (all features)	0.85	1.7

H Sensitivity to Inflation

Our inflation strategy critically impacts the trade-off between risk control and efficiency, requiring careful calibration to maintain statistical validity while avoiding excessive conservatism. Systematic evaluation across inflation levels reveals that our default strategy (1.3× variance inflation, 1.5× slack inflation) effectively balances these competing objectives.

The aggregate results across all datasets demonstrate clear trends in empirical risk reduction as inflation increases. Without inflation, average empirical risk reaches 0.131 ± 0.018 , substantially exceeding our target $\delta = 0.1$. Light inflation (1.15×, 1.2×) provides partial improvement to 0.098 ± 0.013 , while our default strategy achieves 0.084 ± 0.009 , comfortably below the target with reasonable variance. Heavy inflation (1.5×, 2.0×) further reduces risk to 0.069 ± 0.007 but at significant efficiency cost, making the default strategy optimal for practical deployment.

Table 14: Empirical risk vs. inflation factors (mean \pm std across datasets).

Inflation	v factor	η factor	Avg Emp Risk
None	1.0	1.0	0.131 ± 0.018
Light	1.15	1.2	0.098 ± 0.013
Default	1.3	1.5	0.084 ± 0.009
Heavy	1.5	2.0	0.069 ± 0.007

Per-dataset analysis confirms consistent benefits of default inflation across diverse domains, with all datasets achieving empirical risk below the 0.1 target when inflation is applied, compared to systematic violations without inflation. The effectiveness proves particularly pronounced for challenging datasets like ASQA and LegalBench, where complex reasoning patterns benefit most from conservative parameter estimation.

Table 15: Per-dataset risk: default inflation vs. none.

Dataset	No Inflation	Default	Target
GSM8K	0.124	0.083	0.10
HotpotQA	0.138	0.091	0.10
ASQA	0.147	0.098	0.10
TruthfulQA	0.119	0.077	0.10
ProofWriter	0.112	0.069	0.10
LegalBench	0.145	0.089	0.10

These results demonstrate that default inflation provides robust risk control across all datasets, with empirical risk consistently below target levels compared to systematic violations without inflation.

I Expanded Experimental Results

Table 16 provides a systematic comparison of Sequential-EDFL against prior stopping methods across key dimensions.

The gate reduces the HighLift+Incorrect rate by 41% (from 18.5% to 10.9%) with modest TPCA increase (+7.1 tokens) and overhead growth (+4%, Table 17), narrowing the sufficiency–correctness gap while preserving anytime-valid guarantees. The 83% verification reduction is computed as follows: the gate successfully validates 83% of EDFL stopping decisions (Table 17), requiring full verification only for the 17% of stops that fail the gate plus any sequences that continue past EDFL’s threshold.

Table 16: Method comparison: formal guarantees and efficiency.

Method	Formal Guarantee	Anytime Valid	Skeleton-Free	Tokens Saved	Overhead (%)	Tuning Required
Fixed-length	✗	✗	✓	0	0%	None
Entropy threshold	✗	✗	✓	17	3%	τ_H
Conformal stopping	✓	✗	✓	25	8%	Calibration set
SelfCheck	✗	✗	✓	32	22%	Temperature
E-Value	✓	✓	✗	37	16%	λ, μ
Sequential-EDFL	✓	✓	✗	61	12%	None*

*Skeleton construction required but parameters auto-tuned via mixture e-processes

**Tokens Saved computed as average reduction vs. 150-token fixed-length baseline

Table 17: Hybrid gate effect (GSM8K + HotpotQA + ASQA, $n = 500$ each, $\delta = 0.1$).

Setting	Acc	HighLift+Incorrect	TPCA	Ovhd
EDFL (base)	76.8%	18.5%	90.7	12%
+ Sentence boundary only	79.6%	14.7%	93.2	13%
+ Boundary + verifier	83.4%	10.9%	97.8	16%

Verifiers: Arithmetic checker (GSM8K), retrieval overlap ≥ 0.3 (HotpotQA/ASQA)Table 18: Open-ended tasks: dialogue (Wizard, $n = 300$) and summarization (CNN/DM, $n = 300$).

Task	TPCA	Perplexity	ROUGE-L	Human Pref
<i>Wizard-of-Wikipedia (dialogue)</i>				
Fixed-length (150 tok)	150.0	12.3	-	-
EDFL (context ablation)	118.4 \pm 8.7	13.1	-	58%
<i>CNN/DailyMail (summarization)</i>				
Fixed-length (80 tok)	80.0	18.7	0.412	-
EDFL (temperature $\tau = 1.8$)	72.3 \pm 6.2	19.4	0.398	54%

J Proofs

We provide formal proofs for the key theoretical results underlying our Sequential-EDFL framework, establishing the validity of optional skipping and adaptive reset mechanisms within our statistical testing framework.

Proof. The proof of Lemma 3.2 establishes that optional skipping preserves the supermartingale property essential for statistical validity. Because our gate only waits (never triggers sooner), it cannot inflate Type-I error; it only trades a few tokens for better correctness. Formally, optional stopping for nonnegative supermartingales plus the fact that the gate only *delays* stopping (never advancing) implies validity is unchanged. See, e.g., time-uniform concentration via e-processes (Howard et al., 2021a; Vovk and Wang, 2021b; Waudby-Smith and Ramdas, 2023). When $\hat{s}_t = 1$ triggers skipping, we set $X_t = 0$, yielding $\tilde{Z}_t = 0 - \hat{\mu}_{t-1} \leq 0$ since $\hat{\mu}_{t-1} \geq 0$ (all $X_i \geq 0$). For $\lambda > 0$ and $\tilde{Z}_t \leq 0$, the conditional expectation $\mathbb{E}[\exp(\lambda \tilde{Z}_t) | \mathcal{F}_{t-1}] = \exp(\lambda \tilde{Z}_t) \leq 1 \leq \exp\left(\frac{\lambda^2(\hat{\nu}_{t-1} + \eta)}{2(1-c\lambda)}\right)$ remains bounded by our penalty function. The e-process update $\mathbb{E}[M_t | \mathcal{F}_{t-1}] = M_{t-1} \cdot \mathbb{E}[\exp(\lambda \tilde{Z}_t - \psi_t(\lambda)) | \mathcal{F}_{t-1}] \leq M_{t-1}$ preserves the supermartingale property, and by op-

tional stopping theorem (since $\hat{s}_t \in \mathcal{F}_{t-1}$), Theorem 3.1 continues to hold. \square

The proof of Theorem 3.3 extends validity to adaptive segment budgeting by defining segment-wise e-processes $M_t^{(j)} = \sum_k w_k \exp\left(\lambda_k \sum_{i \in [t_j, t]} \tilde{Z}_i - \sum_{i \in [t_j, t]} \psi_i(\lambda_k)\right)$ where each segment j satisfies $\mathbb{P}\left(\sup_t M_t^{(j)} \geq 1/\delta_j\right) \leq \delta_j$ by Theorem 3.1. Within segment j , apply Theorem 3.1 with budget δ_j . Union bound over segments yields $\sum_j \delta_j = \delta$. Since δ_j decays as j^{-2} , the series converges. This is a standard convergent-series budget allocation; cf. segment-wise testing with e-processes (Howard et al., 2021a; Ramdas et al., 2023). The union bound over segments yields $\mathbb{P}\left(\exists j, t : M_t^{(j)} \geq 1/\delta_j\right) \leq \sum_{j=1}^{\infty} \delta_j = \sum_{j=1}^{\infty} \frac{6\delta}{\pi^2 j^2} = \delta$, completing the proof that adaptive resets maintain overall error control at level δ .

K Computational Overhead Breakdown

Detailed profiling of Sequential-EDFL reveals that the 12.1% computational overhead stems primarily from skeleton logit computation, which dominates at 6.5% of baseline generation time. The remaining components contribute modestly: e-process computation across 12 λ values adds 2.1%, drift estimation contributes 1.2%, information lift calculation requires 1.0%, entropy-slope computation adds 0.8%, and EMA updates consume 0.6%. This breakdown suggests optimization opportunities through skeleton caching or distilled models for the dominant component.

Table 19: Overhead breakdown per 100 tokens (LLaMA-2-7B, A100, 1000 runs).

Component	Time (ms)	% of baseline
Baseline generation	520 ± 18	–
Skeleton logits	34 ± 4	6.5%
Lift X_t	5 ± 1	1.0%
EMA updates ($\hat{\mu}, \hat{v}$)	3 ± 1	0.6%
E-process (12 λ s)	11 ± 2	2.1%
Entropy-slope	4 ± 1	0.8%
Drift estimator	6 ± 1	1.2%
Total overhead	63 ± 6	12.1%

L Error Categorization

Analysis of Sequential-EDFL’s error patterns reveals well-calibrated behavior consistent with our theoretical framework. Early stopping (false positive) rates range from 6.1% (ProofWriter) to 11.4% (LegalBench), aligning closely with our target $\delta = 0.10$ after accounting for conservative inflation. Late stopping (false negative) rates remain low at 2.9-6.3%, while timeout events occur rarely at 1.4-2.4%. The higher early stopping rates on complex datasets like LegalBench reflect appropriate conservatism in challenging domains where information accumulation patterns prove more variable.

Table 20: Error distribution for Sequential-EDFL ($\delta = 0.1$) across datasets.

Dataset	Correct	Early (FP)	Late (FN)	Timeout
GSM8K	87.9%	7.3%	3.2%	1.6%
HotpotQA	82.7%	9.4%	5.6%	2.3%
ASQA	81.2%	10.3%	6.1%	2.4%
TruthfulQA	85.8%	8.1%	4.4%	1.7%
ProofWriter	89.6%	6.1%	2.9%	1.4%
LegalBench	79.9%	11.4%	6.3%	2.4%

M Reproducibility Checklist

Our experiments ensure full reproducibility through systematic control of randomness and computational environment. Random seeds are fixed across all frameworks: NumPy uses seed 42, PyTorch uses seed 123, and Python’s random module uses seed 789. CUDA operations employ deterministic mode via `torch.use_deterministic_algorithms` to eliminate non-deterministic GPU computations. All datasets include SHA-256 checksums provided in supplementary material for integrity verification.

The experimental setup employs three language models: LLaMA-2-7B (`meta-llama/Llama-2-7b-hf`), LLaMA-2-13B (`meta-llama/Llama-2-13b-hf`), and GPT-4 (`gpt-4-0613`). Retrieval-augmented generation experiments use Contriever-MS MARCO with top-5 retrieval and maximum 512 tokens per document. The computational environment consists of 4×A100 (40GB) GPUs running CUDA 11.8 and PyTorch 2.0.1. All hyperparameters are comprehensively documented in Table 5, and complete source code will be released upon acceptance to ensure full experimental replication.

N Algorithmic Specification

This algorithm provides a complete, executable specification of Sequential-EDFL, integrating self-normalized e-processes (lines 13-17), mixture combination (line 18), anytime-valid stopping (lines 20-22), and adaptive drift handling (lines 24-28). The computational complexity is $O(K)$ per token for K parameters, achieving 12% overhead with $K = 12$ in our experiments.

Algorithm 1 Sequential-EDFL algorithm with optional correctness gate.

Require: Input x , error rate δ , skeleton model S , parameter grid $\{\lambda_1, \dots, \lambda_K\}$

```
1: Initialize: segment  $J \leftarrow 1$ ,  $M_t(\lambda_k) \leftarrow 1$  for all  $k$ ,  $\hat{\mu} \leftarrow 0$ ,  $\hat{v} \leftarrow 0$ ,  $\alpha \leftarrow 0.1$ 
2: Set budget  $\delta_J \leftarrow 6\delta/(\pi^2 J^2)$ , threshold  $u_J \leftarrow 1/\delta_J$ 
3: for  $t = 1, 2, \dots$  do
4:   Sample  $y_t \sim P(\cdot|x, y_{1:t-1})$  from full model
5:   Compute skeleton probability  $s_t \leftarrow S(y_t|x, y_{1:t-1})$ 
6:   Compute full probability  $p_t \leftarrow P(y_t|x, y_{1:t-1})$ 
7:   Compute lift:  $X_t \leftarrow \log(p_t/s_t)$  ▷ Bounded to  $[0, c]$  via clipping
8:   // Optional Skipping
9:   if entropy slope  $H_{t-1} - H_{t-2} \geq 0$  then continue ▷ Skip high-uncertainty steps
10:  end if
11:  // Update EMA Estimates
12:   $\hat{\mu} \leftarrow (1 - \alpha)\hat{\mu} + \alpha X_t$ 
13:   $\hat{v} \leftarrow (1 - \alpha)\hat{v} + \alpha(X_t - \hat{\mu})^2 + \eta$  ▷  $\eta$ : inflation for conservatism
14:  // Update E-Processes for Each Parameter
15:  for  $k = 1, \dots, K$  do
16:     $M_t(\lambda_k) \leftarrow M_{t-1}(\lambda_k) \cdot \exp\left(\lambda_k(X_t - \hat{\mu}) - \frac{\lambda_k^2 \hat{v}}{2}\right)$ 
17:  end for
18:  // Mixture E-Process
19:   $M_t \leftarrow \sum_{k=1}^K w_k M_t(\lambda_k)$  where  $w_k = 1/K$  ▷ Uniform mixture
20:  // Stopping Decision
21:  if  $M_t \geq u_J$  then
22:    // Optional gate: only DELAYS stopping; never advances it (Lemma 3.2)
23:    if  $\text{IsSentenceBoundary}(y_{1:t})$  and  $\text{VerifierPass}(x, y_{1:t}) \geq \tau_c$  then
24:      return  $y_{1:t}$  ▷ Stop: info sufficient & gate passed
25:    else
26:      continue ▷ Delay stopping until boundary+verifier pass
27:    end if
28:  end if
29:  // Drift Detection
30:  Compute drift statistic  $\hat{d}_t \leftarrow |\hat{\mu}_{\text{recent}} - \hat{\mu}_{\text{overall}}|$ 
31:  if  $\hat{d}_t > \tau_d$  then
32:     $J \leftarrow J + 1$ , reset  $M_t(\lambda_k) \leftarrow 1$  for all  $k$ 
33:    Update budget  $\delta_J \leftarrow 6\delta/(\pi^2 J^2)$ , threshold  $u_J \leftarrow 1/\delta_J$ 
34:  end if
35: end for
```

O Extended Related Work

Sequential-EDFL builds upon sequential testing theory, particularly e-processes (Vovk and Wang, 2021a; Ramdas et al., 2023; Howard et al., 2021a) that provide anytime-valid inference with roots in Ville’s martingale theory (Ville, 1939) and modern confidence sequences (Robbins, 1970; Lai, 1976; Howard et al., 2021b). Self-normalized e-processes (Howard et al., 2021a; Waudby-Smith and Ramdas, 2023) handle unknown centering via running variance estimation, directly inspiring our empirical-Bernstein extension. Recent work on sequential inference in LLMs (Lew et al., 2023) demonstrates the value of adaptive stopping, though without anytime-valid guarantees. Safe testing (Grünwald et al., 2019) and betting scores (Waudby-Smith and Ramdas, 2021) provide additional theoretical grounding and baseline comparisons for our anytime-valid framework.

Conformal prediction represents a complementary approach to uncertainty quantification that offers finite-sample guarantees through split conformal methods (Vovk et al., 2005; Angelopoulos and Bates, 2021), though requiring calibration sets. Extensions encompass conformalized quantile regression (Romano et al., 2019), distribution-free inference (Lei et al., 2018), and covariate shift adaptation (Tibshirani et al., 2019), with online variants (Gibbs and Candes, 2021) and time series extensions (Darrin and Tibshirani, 2023) addressing distribution shift. However, these approaches don’t naturally accommodate token-level stopping decisions in sequential generation, motivating our e-process framework.

Within the LLM uncertainty landscape, existing approaches include entropy-based methods (Malinin and Gales, 2018), semantic consistency checks (Manakul et al., 2023), verbalized confidence (Kadavath et al., 2022), and hallucination detection (Varshney et al., 2023; Fadeeva et al., 2024), yet these lack the formal statistical guarantees that our framework provides through frequentist control with anytime-valid error rates. Risk-aware decoding encompasses constrained generation (Hokamp and Liu, 2017), calibration techniques (Guo et al., 2017; Minderer et al., 2021; Kumar et al., 2019), and selective abstention (Geifman and El-Yaniv, 2017) using static thresholds, alongside out-of-distribution detection (Hendrycks and Gimpel, 2017; Liang et al., 2018; Lee et al., 2018) for uncertainty estimation. Our work extends

this paradigm by providing sequential, anytime-valid control that dynamically adapts to evidence accumulation patterns.

Information-theoretic metrics in NLP (Meister et al., 2021; Sachan et al., 2021) inform our lift construction, though prior work lacks the statistical testing frameworks necessary for principled stopping decisions with formal guarantees. Recent advances in reasoning (Wei et al., 2022; Kojima et al., 2022; Wang et al., 2023), tool use (Schick et al., 2023; Yao et al., 2022; Chen et al., 2022), and retrieval-augmented generation (Lewis et al., 2020; Karpukhin et al., 2020; Borgeaud et al., 2022) demonstrate both the importance of controlled generation and the need for measuring information gain from external sources, directly motivating our skeleton-based approach to quantifying evidence accumulation.